SUSTAINABLE WASTE-TO-WEALTH INNOVATION EXPLORING THE POTENTIAL OF BINDERLESS PAPER-BASED COMPOSITE BOARDS AS CEILINGS FOR BUILDING CONSTRUCTION

INNOVACIÓN SOSTENIBLE DE RESIDUOS A RIQUEZA: EXPLORACIÓN DEL POTENCIAL DE TABLEROS COMPUESTOS DE PAPEL SIN ADHESIVO COMO CIELOS RASOS PARA LA CONSTRUCCIÓN DE EDIFICIOS

Ubong Williams Robert[1], Sunday Edet Etuk[2], Okechukwu Ebuka Agbasi[3*]

[1] Department of Physics, Faculty of Physical Sciences, Akwa Ibom State University, Ikot Akpaden, Mkpat Enin, Nigeria.

[2] Department of Physics, Faculty of Physical Sciences, University of Uyo, Uyo, Nigeria.

[3] Okna Geophysical Services, Eket, Nigeria.

(Received: apr./2025. Accepted: jun./2025)

Abstract

In this research, binderless paper-based composite boards were fabricated from waste papers and then assessed experimentally for their suitability as ceiling materials in building construction. During the process, waste newspaper paste (WNP) and waste writing paper paste (WWP) were prepared and used at varying percentages (0, 30, 50, 70, and 100%) on weight basis to develop the ceiling samples. Three samples were prepared for each mix design, dried to constant weight, and characterized in terms of physical properties, thermal responses, and strength behaviors. The results showed maximum bulk density (587.0 kgm^{-3}), thermal conductivity (0.0835 $Wm^{-1}K^{-1}$), thermal diffusivity (10.56 x 10^{-8} m^2s^{-1}), flexural strength (1.318 N/mm^2), and internal bond strength (0.214 N/mm^2) at 100.0% loading of the WWP. Though

* agbasi.okechukwu@gmail.com https://doi.org./10.15446/mo.n71.119616

nailability remained 100.0% notwithstanding the composite mixes, the samples recorded the highest thickness swelling (26.89%), void fraction (49.92%), and specific heat capacity (1429 $Jkg^{-1}K^{-1}$) as the proportion of the WNP increased to 100.0%. Further, it was found that these WNP-WWP samples could outperform conventional ceilings such as plaster of Paris, asbestos, and KalsiCeil. The undertaking described herein can ensure reduction in production time since no adhesive is required, thus benefiting both the environment and economy while availing the building sector with cost-effective and sustainable ceilings for building construction. The knowledge from this research could help in solving the disposal problems associated with waste papers and also tackling hampering of sustainable housing development due to high cost of building construction materials.

Keywords: bulk density, flexural strength, thermal comfort, thermal insulation, waste recycling.

Resumen

En esta investigación, se fabricaron tableros compuestos de papel sin adhesivo a partir de papel de desecho, y luego se evaluó experimentalmente su idoneidad como materiales para cielos rasos en la construcción de edificios. Durante el proceso, se prepararon pasta de periódico reciclado (WNP, por sus siglas en inglés) y pasta de papel de escritura reciclado (WWP), las cuales se utilizaron en diferentes proporciones (0, 30, 50, 70 y 100 %) con base en el peso para desarrollar las muestras de cielo raso. Se prepararon tres muestras para cada diseño de mezcla, manteniendo un peso constante, y se caracterizaron en términos de propiedades físicas, respuestas térmicas y resistencia mecánica. Los resultados mostraron una densidad máxima aparente de 587,0 kg m^{-3}, conductividad térmica de 0,0835 $Wm^{-1}K^{-1}$, difusividad térmica de 10.56 x 10^{-8} m^2s^{-1}, resistencia a la flexión de 1,318 N/mm^{-2} y resistencia interna a la tracción de 0,214 N/mm^{-2} a una proporción del 100 % de WWP. Aunque la resistencia a la tracción interna se mantuvo en 100,0 % a pesar de las mezclas compuestas, las muestras registraron el mayor hinchamiento por absorción (26,89 %), fracción de vacíos

(49,92 %) y capacidad calorífica específica (1429 $Jkg^{-1}K^{-1}$) a medida que la proporción de WNP aumentó hasta el 100,0 %. Además, se encontró que las muestras WNP-WWP podrían superar a los cielos rasos convencionales como los de yeso de París, asbesto y KalsiCeil. El proyecto descrito aquí garantiza una reducción en los costos de producción, ya que no se requiere adhesivo, beneficiando así tanto al medio ambiente como a la economía, y proporcionando al sector de la construcción una solución rentable y sostenible para los cielos rasos. El conocimiento generado en esta investigación podría ayudar a resolver los problemas de disposición de papel de desecho y, además, a contrarrestar los obstáculos para el desarrollo de viviendas sostenibles debido al alto costo de los materiales de construcción tradicionales.

Palabras clave: densidad aparente, resistencia a la flexión, confort térmico, aislamiento térmico, reciclaje de residuos.

1. Introduction

The rapid increase in the world's human population witnessed in recent times has necessitated intensification of efforts towards reduction in energy need of a building and improvement of indoor environment quality. Essentially, a decent home is a fundamental human need [1, 2] and the key purpose of constructing a building is to provide a comfortable temperature range for its occupants, thereby contributing to their overall well-being and productivity within the space [3]. All these are in line with the agenda of Sustainable Development Goal (SDG) which emphasize on ensuring that everyone has access to safe, adequate, and affordable housing by 2030. In designing a building, ceiling is a vital part to be considered for thermal insulation and aesthetic appeal of the indoor environment. It is obvious that achievement of the SDG through dependence on conventional ceiling materials (some of which are plywood, Isorel, polyvinyl chloride, plaster of Paris, etc) is unfeasible due to certain factors one of which is high cost of building materials [4]. Another factor is heatwaves caused by climate change leading to creation of vicious cycle in the environment, thus posing increased risks on human health and overall quality of life [5]. To overcome the above-mentioned challenges, research interest is nowadays

surged in promoting environmentally conscious products within the building industry, with notable focus on utilization of waste items for ceilings production. This is clearly a circular economy approach and, by rethinking design, construction, and material usage, the building industry can dramatically reduce its ecological footprint.

Wastepaper is a typical recyclable material for such purpose and utilizing it offers additional advantage in terms of availability and sustainability. This is because paper is a necessity of civilization and so, there can be no halt in its production as well as generation of the resulting waste [6]. In a year, over 300 million tons of papers are used globally [7] and 100 million tons of waste papers are generated [8]. Amena et al. [9] utilized wastepaper, sawdust, recycled polyethylene terephthalate, and epoxy resin to fabricate ceiling tiles. Okorie et al. [10] produced composite ceiling panels from waste carton papers and tiger nut fiber with cassava starch slurry as binding agent. Ibrahim et al. [11] developed composite ceiling board materials from rice husk, rice husk ash, and wastepaper with Urea Formaldehyde glue as binder for use in low-cost construction work. Utilization of sawdust with waste newspaper, writing - paper, and carton paper with cassava starch slurry as binding agent for production of ceiling boards was demonstrated [12]. The use of waste carton and *Musanga cecropioides* heartwood particles with epoxy as binder to produce composite ceiling panels was reported [13].

It is noteworthy that though binders basically act as glue that holds the composite ceiling components together, their utilization has demerits as well. For instance, synthetic binders (cement, epoxy resin, acrylic, phenol formaldehyde, polyvinyl chloride, malemine, urea formaldehyde, etc) can have disadvantages including environmental impact, cost, and health concerns. Also, natural binders (starches, gums, mucilages, dried fruits, etc) can cause processing issues and are prone to microbial contamination and changes in viscosity. Moreover, under-utilization of waste papers warrants adoption of open incineration for their prevalent disposal due to persistence of ineffective/limited solid waste management systems in less-developed and developing countries. This practice contributes to environmental pollution by releasing harmful air pollutants like carbon monoxide, particulate matter, and nitrogen oxides into atmosphere making it very detrimental [14, 15, 16]. Obviously, there is an urgent need to consider how to address the above-identified socio-economic challenges for the benefits of humans.

For instance, Sassanelli et al. [17] noted that minimization of material wastage and maximization of the reuse of resources could streamline building construction process and lower the associated cost.

Therefore, the aim of this research is to produce binderless composite panels from waste papers and then determine their suitability as ceiling materials in building construction. Aside combining waste papers only to develop the new products, non-utilization of any adhesive is another novel aspect that not only makes this research uniquely innovative but also advantageous over the afore-mentioned cases of composite ceilings fabrication using waste papers. Specifically, appraisal of the panels' performance for the intended application will be with regard to their physical properties, thermal responses, and strength behaviors relevant to the purpose. Zhang et al. [18] demonstrated a facile and efficient approach to prepare adhesive-free all-lignocellulosic composites with excellent performances via the dialdehyde modification. Ju et al. [19] reported an effective method for making adhesive-free biomass composites using a strategy involving selectively oxidizing biomass in situ, followed by adhesive-free bonding through one-step molding. Nitu et al. [20] presented an overview on binderless particleboard's development from different agricultural wastes using an assorted range of manufacturing processes and their self-bonding mechanisms. A study by Anukam et al. [21] on how to improve the understanding of bonding mechanism of primary components of biomass pellets through the use of advanced analytical instruments revealed that, at a microscopic level, solid bridges caused by intermolecular bonding from highly electronegative polar functional groups linked to cellulose and hemicelluloses. It is hoped that as this study seeks to further explore how to safely manage waste papers by utilizing them to enhance sustainable housing development, findings from it would add value to circular economy and greatly benefit building engineers, researchers, architects, materials scientists, environmentalists, and waste managers.

2. Experimental Arrangement

2.1 Materials Description and Acquisition

Newspapers and writing papers discarded as waste items were the main materials used in this research. The waste newspapers consisted of five popular Nigerian Dailies (named The Nation, Punch, Vanguard, Guardian,

and Daily Post) produced using the same quality of newsprint. Used graph sheets and leaves of exercise books were the waste writing papers utilized also in this research. The waste newspapers were collected from paper vendors while the waste writing papers were picked from the dumpsites at various educational institutions. Each wastepaper type was gathered in large quantity within Uyo metropolis, Akwa Ibom State, Nigeria.

2.2 Particulars of Wastepaper

Since papers vary in quality and weight which in turn influence their choice for application [22], it was deemed necessary to determine the thickness and grammage of the waste papers in order to provide further insights into the distinctiveness of their types. In doing so, a digital micrometer screw gauge was used to measure the thicknesses of the waste papers. Also, ten precise circular pieces were cut from each paper and weighed singly using a digital weighing scale. The grammage (in gram per square meter) of each paper piece was determined by applying the formula

$$P_G = \frac{W}{A_p} \tag{1}$$

where P_G = paper grammage, W= weight of a paper piece, and A_p= area of the paper piece.

2.3 Processing of Wastepaper

The gathered papers were surface-cleaned (to remove any accompanying dirt and other unwanted items from them) and sorted according to their types (waste newspapers and waste writing papers) before shredding and soaking them separately in potable water initially at 28 ^{o}C. After 18 hours, each soaked material was removed from the water, lightly squeezed, and then pounded into paste using Agate mortar and pestle. The waste newspaper paste (WNP) and waste writing paper paste (WWP) were sufficiently sun-dried, ensuring that they became moisture-free.

2.4 Chemical Analyses of the WNP and WWP

The lignocellulosic constituents (cellulose, hemicellulosic, and lignin) of the WNP were analyzed and quantified by adopting the Technical Association of the Pulp and Paper Industry protocols. Accordingly,

the proportion of lignin was determined using gravimetric technique in compliance with the standard TAPPI T222 (Acid-insoluble lignin in Wood and Pulp) after the removal of extractives following the procedures outlined in TAPPI T204 (Solvent extractives of Wood and Pulp). The holocellulose content was determined as per the stipulations in TAPPI T249 (Cellulose in Pulp) followed by quantification of the cellulose based on TAPPI T203 (Alpha, Beta, and Gamma-cellulose in Pulp). By calculating the difference between the holocellulose and cellulose contents, the proportion of hemicellulose was obtained. All the analyses were performed five times and similar procedural steps were followed to determine the chemical compositions of the WWP.

2.5 Fabrication of the Paper-based Boards

The WNP and WWP were mixed at various varying proportions (such as 0, 30, 50, 70, and 100%) on a dry weight basis and the mixes were moistened with potable water. For each design, 2:1 ratio by weight of the water to material mix was used throughout the moistening stage. The moistened mixtures were cast in molds and compacted using a laboratory-made compacting machine maintained at 10 kN. Prior to casting, the inner edges of the molds were properly covered with cellophane material for ease of demolding. After 24 hours, the pressed materials were demolded and dried under intense sunlight for several days until a constant weight was achieved in each case. Samples meant for appraisal of physical properties and thermal responses were developed in molds with thickness of 8 mm measuring 110 mm in diameter while the ones for assessment of strength characteristics were formed in molds of dimensions 540 mm × 80 mm × 20 mm. The samples were fabricated in triplicate and used for the tests as intended. Figure 1 summarizes the fabrication processes for the samples in this research.

FIGURE 1. *Summary of the sample's fabrication processes*

2.6 Testing of the Samples

2.6.1 *Physical Properties*

Bulk density

Bulk density was assessed to gain insight into the heaviness, or otherwise of the samples. In this study, the sample under test was weighed by means of a digital balance (capable of reading up to 0.1 g) and its bulk volume was determined by Modified Water Displacement method, and it was adopted as detailed in [23]. Using paraffin wax, the entire sample's surfaces were sealed to prevent water intrusion during the test. When the coated sample was completely immersed in water in a glass measuring cylinder, the displacement of the water was measured using digital vernier callipers and then used to find the volume of the coated sample. The bulk density of the sample was obtained in accordance with the relation

$$\rho = \frac{M_s}{(V_c - V_p)} \tag{2}$$

where ρ= bulk density, M_s= mass of the sample, V_c= volume of the coated/sealed sample (volume of the displaced water), and V_p= volume of the sealant on the sample under test.

Thickness swelling

This property was evaluated to provide useful information on the dimensional stability of the boards with regard to their intended application since they might be prone to be attacked by water during leakage of roofing materials in a building. The thickness swelling test was performed using water immersion method [13, 24]. Each sample's thickness was measured with the callipers and noted before the samples were immersed completely in water and then allowed to remain in that condition for 24 hours. After the submersion period, the samples' surfaces were quickly dabbed with absorbent paper (to remove the excess water) followed by measurement of their final thicknesses. Using the data obtained, the thickness swelling was computed as

$$T_s = \left(\frac{T_f - T_i}{T_i}\right) 100\% \tag{3}$$

where T_s= thickness swelling, T_i= thickness of the sample prior to the immersion, and T_f= sample's thickness after the immersion.

Void fraction

Since the samples are porous, there exist empty spaces in them which affect their behaviors, thus making void fraction a very crucial consideration for understanding of the samples' performances through characterization of their pore geometry. In this research, the void fraction was quantified by employing a gas pycnometer (Model G-DenPyc 2900) [25]. The samples were cut to regular shape and with appropriate size enabling the determination of their volume with ease. Next, the sample to be tested was placed in the chamber of the pycnometer and sealed. As helium gas was introduced into the system, the mixture was agitated very gently and carefully, maintaining the temperature of the

compartment until the pressures equilibrated. The volume of gas in the sample was applied to calculate the void fraction, V_f of the sample according to the equation

$$V_f = \left(\frac{V_a}{V_s}\right) 100\% \tag{4}$$

where V_a= total void (volume of gas) in the sample, and V_s= volume of the sample under test.

2.6.2 *Thermal responses*

Thermal conductivity

The thermal conductivity of each sample was determined using Modified Lee-Charlton's Disc apparatus technique [26]. Figure 2 shows the setup used for this aspect of experimentation. Each disc measured 110 mm in diameter and was equipped with a calibrated digital thermometer (Model 305) employing type-k probe for temperature sensing/measurement. An electric hotplate (Model E4102WH) was used as the heat source. The thickness of the sample and that of the upper disc were properly and thickly lagged with cotton wool. When the system attained a steady state, the temperature of each disc was noted, and temperature-time cooling data were generated. The data were then graphed and modeled using Origin Software (Version 2019b) to establish temperature as a function of time which permitted the determination of the rate of cooling as described in [27]. Applying the relevant data, the thermal conductivity of the sample was calculated as

$$k = \left(\frac{Mcx}{A\Delta\theta}\right)\frac{dT}{dt} \tag{5}$$

where k= sample's thermal conductivity, M= mass of the upper disc, c= specific heat capacity of the disc, x= theickness of the sample, A= area of the cross-section of the sample, $\Delta\theta$= difference between the temperatures of the discs at steady state, and $\frac{dT}{dt}$= rate of cooling of the disc.

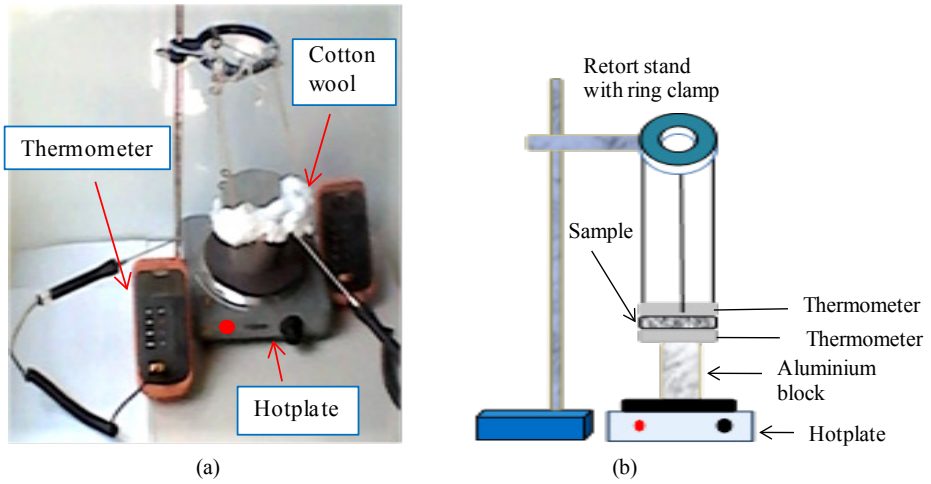

FIGURE 2. *Setup for the thermal conductivity determination (a) Experimental (b) Schematic*

Specific heat capacity

SEUR'S apparatus was used for the purpose of determining the specific heat capacity of the samples [28]. Figure 3 shows the views of the apparatus. In addition to the plate of the sample to be tested, other heat exchange accessories were brown plywood plate and aluminium plate each of which measured 60 mm × 60 mm × 8 mm. After being heated to about 65 °C, the aluminium plate was quickly and carefully sandwiched between the plywood and sample, all of which were enclosed within the cavity of the device. Immediately, their temperatures were noted and observed afterwards until no further change was noticed in each case indicating that thermal equilibrium was reached by the system. At that instant, the total quantity of heat gained by the sample and plywood plates was determined and the amount of heat lost by the aluminium plate was also calculated. With the assumption that heat energy was conserved, the specific heat capacity of the sample was computed using the formula

$$C = \left(\frac{Q_a - q}{M_b \Delta T}\right) \tag{6}$$

where C= specific heat capacity, Q_a= quantity of heat lost by the aluminium plate, q= quantity of heat gained by the plywood plate, M_b= mass of the sample, and ΔT= change in temperature of the sample.

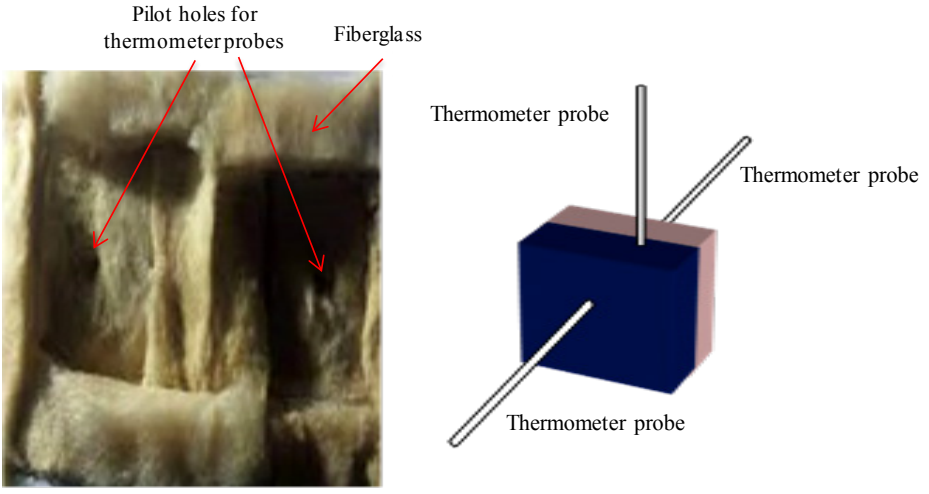

FIGURE 3. *Views of the SEUR'S apparatus (a) Internal (b) Schematic*

Thermal diffusivity

Based on the bulk density, thermal conductivity, and specific heat capacity already obtained for each sample, the corresponding thermal diffusivity was determined using the formula applied by several researchers including [249- 34] as

$$\lambda = \frac{k}{\rho C} \tag{7}$$

where λ= thermal diffusivity.

2.6.3 Strength behaviors

Nailability

This test was necessary to examine the samples' ability to withstand nailing in the course of their installation in buildings. In was performed by

using a nail gun named Finish Nailer (Model D51257K, manufactured by Dewalt) to hammer a 2"- nail through the thickness of a sample at a time [12]. The sample was placed on a softwood board during the test and the hammering operation carried out slowly and methodically. Figure 4 shows a typical nailing process of the sample. When a tiny visible crack was noticed or the nail tip appeared on the opposite side of the sample, the operation was discontinued, and the depth of the nail penetration was determined as the difference between the overall length of the nail and the length of the remaining nail portion. For an operation devoid of any visible crack, the penetration depth of the nail was considered to be the same as the thickness of the sample under test. In either case, the nailability was obtained as [24]

$$n_b = \left(\frac{H - h}{x}\right) 100\% \tag{8}$$

where n_b= nailability, H= overall length of the nail, x= sample's thickness, and h= length of the remaining portion of the nail at the discontinuation of the nailing.

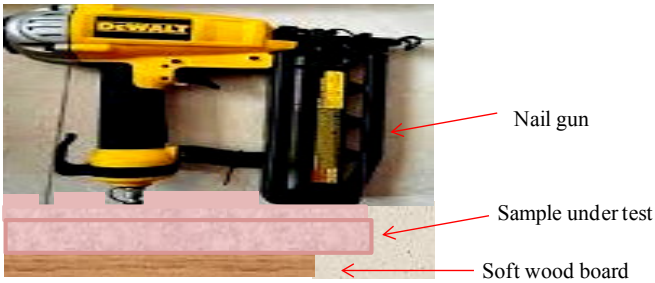

FIGURE 4. *A view of the nail gun under use*

Flexural strength and Internal bond strength

These properties were assessed with the aid of a universal testing machine (H10kT) based on the protocols documented in ASTM D1037 [35]. For evaluation of the flexural strength, the samples were carefully cut to measure 530 mm × 76 mm × 20 mm in size and one sample was tested in each schedule using three-point bending technique. The sample was placed on the flexure assembly of the machine as illustrated in Figure 5 and loaded centrally with a 10kN-load cell at 4 mm/min

until it failed flexurally. At that instant, the maximum applied force was noted and the flexural strength was calculated as [36]

$$f_s = \frac{3}{2}\left(\frac{Fd}{bx^2}\right) \tag{9}$$

where f_s= flexural strength, F= load/force applied when failure occurred, x= sample's thickness, d= span length, and b= width of the sample.

In the case of internal bond strength probing, each of the samples was machined to size 50 mm ×50 mm × 20 mm. The sample was gripped properly to the loading fixtures and stressed perpendicularly to its surface at a uniform rate of 1 mm/min. When the sample was pulled apart, the internal bond strength was calculated using the formula

$$I_B = \frac{P}{bL} \tag{9}$$

where I_B= internal bond strength, P= maximum stress necessary to cause the failure, b= sample's width, and L= length of the sample.

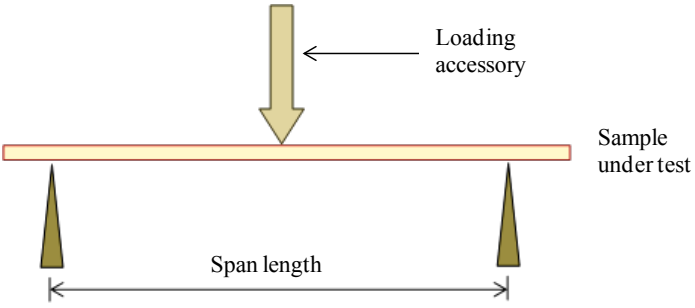

FIGURE 5. *Sample under loading in the machine during strength test*

3. Results and Discussion

3.1 Particulars of Wastepapers

Table 1 shows the thickness and weight of the waste papers utilized in this study. It is noticed that the two types of waste papers differ both in thickness and grammages with the waste writing papers being slightly

thicker (14.8%) and also heavier (30.0%) than the waste newspapers. Their grammage is within the typical range of values for each type of paper.

Wastepaper type used	**Average thickness (mm)**	**Grammage (gsm)**	
		Obtained value	**Typical range of values**
Newspapers	0.081	50.0	42.0 – 60.0
Writing papers	0.093	75.0	70.0 – 90.0

TABLE 1. *Particulars of Wastepapers*

3.2 Chemical Compositions of the WNP and WWP

The proportions of lignocellulosic components of the WNP and WWP are presented in Table 2. It can be seen from the results that the WNP is richer in cellulose content only compared to the WWP, indicating that both fibers are capable of exhibiting distinct hygroscopic behaviors. Cellulose, hemicellulose, and lignin contents of the WNP and WWP differ by about 33.2%, 18.7%, and 15.7%. This is possible because the mixture of raw materials used in manufacturing newspapers is not exactly the same as in the case involving the production of the writing papers. For instance, the primary material for making newsprint paper is wood pulp (specifically from softwood) whereas wood pulp from both hardwood and softwood is utilized in addition to additives (like fillers, dyes, pigments) for production of writing papers.

Lignocellulosic constituents	**Proportion (%) per processed material**	
	WNP	**WWP**
Cellulose	81.7 ± 0.1	48.5 ± 0.1
Hemicellulose	10.2 ± 0.2	28.9 ± 0.2
Lignin	5.6 ± 0.1	21.3 ± 0.2

TABLE 2. *Chemical Composition of the WNP and WWP*

3.3 Properties of the Prepared Samples

3.3.1 *Physical Properties*

Table 3 shows the results of the property tests performed on the samples. The samples' bulk densities vary accordingly, decreasing with added proportions of the WNP. This could stem from the fact that the WWP

is heavier than the WNP as substantiated by the grammages of the wastepaper materials from which they are made. However, the samples can be regarded as low-density boards/panels. Compared to conventional ceilings like plaster of Paris, asbestos, and KalsiCeil with bulk density reported as 1487, 1844, and 1265 (each in kgm^{-3}) respectively [25], these samples are less dense. Aside from being inexpensive, their lightweightness can ensure a remarkable reduction in dead loads which would be an additional advantage if they are applied as ceiling boards in buildings.

The thickness of swelling increases as more of the WNP is included in the sample. This may be attributed to the fact that, since cellulose is highly hydrophilic in nature, its higher proportion makes increasing loadings of the WNP to yield samples with greater water absorption which eventually brings about higher thickness swelling. Ferrandez-García et al. [37] reported thickness swelling of 40.0% for 24-hour immersion of binderless particleboards made from Sorghum. Comparatively, the readiness of the samples to absorb water is of lower degree than the Sorghum-based particle boards. The use of low proportion of the WNP enables the sample to have low thickness swelling signifying higher dimensional stability. Utilization of 30.0% WNP yields sample with thickness swelling comparable to maximum value of 21.49% reported by Mitchual et al. [38] for 24-hour immersion of particleboards produced from residues of plantain pseudostem, cocoa pod and stem and *Ceiba* for indoor applications.

Since the samples contain no adhesive and they are completely-dry porous panels, the voids in them are filled by air. The variations in the samples' void fractions may be due to differences in the lignin proportions of the WNP and WWP which primarily depend on the qualities of the respective waste papers utilized. Among the lignocellulosic constituents, lignin is waxy with gluing properties always behaving as natural adhesive in wood products. Because the WWP contains more lignin than the WNP (as a result of the mixture of wood pulp from which it is manufactured), more interstices exist in the WNP allowing larger space for air thus leading to greater void fraction.

Ratio of WNP: WWP (%)	**Physical properties**			**Thermal responses**			**Strength behaviors**		
	ρ (kgm^{-3})	T_s (%)	V_f (%)	k ($Wm^{-1}\ K^{-1}$)	C ($10^3 Jkg^{-1}K^{-1}$)	λ ($10^{-8} m^2 s^{-1}$)	n_b (%)	f_s (N/mm^2)	I_B (N/mm^2)
0:100	587.0 ± 0.5	19.35 ± 0.06	22.61 ± 0.04	0.0835 ± 0.0003	1.346 ± 0.002	10.56 ± 0.04	100.0 ± 0.0	1.318 ± 0.002	0.214 ± 0.002
30:70	562.4 ± 0.4	21.65 ± 0.06	30.69 ± 0.03	0.0774 ± 0.0002	1.368 ± 0.002	10.06 ± 0.04	100.0 ± 0.0	1.301 ± 0.003	0.192 ± 0.001
50:50	547.5 ± 0.4	23.58 ± 0.07	36.21 ± 0.02	0.0724 ± 0.0003	1.385 ± 0.002	9.55 ± 0.04	100.0 ± 0.0	1.276 ± 0.003	0.181 ± 0.001
70:30	532.6 ± 0.5	25.30 ± 0.08	41.77 ± 0.03	0.0679 ± 0.0003	1.407 ± 0.003	9.07 ± 0.04	100.0 ± 0.0	1.249 ± 0.002	0.175 ± 0.001
100:0	519.6 ± 0.4	26.89 ± 0.07	49.92 ± 0.04	0.0628 ± 0.0002	1.429 ± 0.003	8.46 ± 0.03	100.0 ± 0.0	1.235 ± 0.003	0.161 ± 0.002

TABLE 3. *Results of the tests performed on the samples*

3.3.2 *Thermal responses*

Thermal conductivity is a very crucial transport property for evaluation of ceiling's heat insulation performance. For heat-insulating and building construction materials, the recommended values of k range from 0.023 $Wm^{-1}K^{-1}$ to 2.900 $Wm^{-1}K^{-1}$ [39]. The studied samples' thermal conductivities fall within this range. It can be adduced that the most conductive of the samples is about 97.1% better thermally-insulating than the least suitable thermal insulation material for building purposes. Sample made with 50.0% each of the WNP and WWP has the exact thermal conductivity value reported in [12] for panel produced with similar loadings but using sawdust and waste writing papers. Air is a good thermal insulant and its influence on thermal conductivity of a dry porous material is not in doubt. As expected, an inverse relationship is revealed in Figure 6 between the thermal conductivity and void fraction of the samples. Since more air pockets are trapped within the fiber structure of the WNP, the thermal conductivity reduces with increasing proportions of the WNP thus enhancing thermal insulation efficiency of the resulting composite sample.

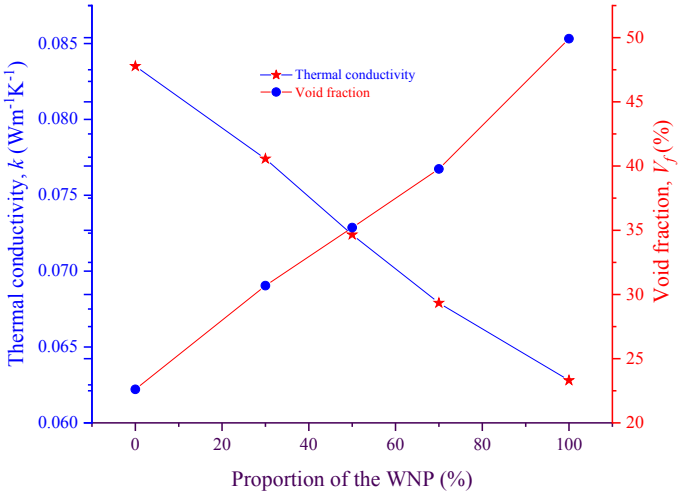

FIGURE 6. *Trend in the samples' thermal conductivity and Void fraction with the WNP content*

Unlike thermal conductivity, the specific heat capacity of the samples increases with increasing percentages of the WNP, indicating greater heat-storing ability. Using up to 70.0% WNP brings about 4.5% marginal increments in specific heat capacity. Noticeably, low thermal conductivity with high specific heat capacity causes low thermal diffusivity of the samples. This observation can be explained in terms of thermal resistance (ratio of thickness to thermal conductivity). As it is, the WNP alone has thermal resistance of 0.127 $W^{-1}m^2K$ which is 32.3% higher than the value of 0.096 $W^{-1}m^2K$ for the WWP. By having a higher specific heat capacity (1424 $Jkg^{-1}K^{-1}$) as well, the WNP exhibits a greater tendency to effectively delay heat diffusion for temperature propagation than the WWP. In hot-temperature regions, materials with such low thermal diffusivity are highly desirable in buildings for thermal comfort of the occupants. This makes the WNP-WWP ceiling samples have a competitive advantage as far as enhancement of thermal comfort is a priority consideration.

3.3.3 *Strength behaviors*

From the results of nailability assessment, it is clear that the samples can be installed successfully as ceilings by nailing. Since cellulose primarily provides strength for fibrous materials, the high content of it in both the WNP and WWP may be responsible for the observed nailability of the samples. The nailability results in this study are similar to the findings by Etuk et al. [24] in the case of composite ceiling panels produced from sugarcane bagasse and waste newspapers with epoxy as binding agent. Not only that, but the least flexural strength value of the samples also exceeds the range of 0.038 N/mm^2 to 1.128 N/mm^2 obtained by Nduduba et al. [40] for particleboards made from Fonio husks with up to 30% Gum Arabic resin as adhesive for interior applications. This means that a square millimeter of the sample with 100.0% WNP will be about 9.5% stronger than the said Fonio husk particleboards in resisting bending stress under same conditions of use.

Internal bonding has a pronounced influence on the flexural strength of a material. In the instant case, the flexural strength and internal bond strength of the samples exhibit decreasing trend with proportion of the WNP. Internal bond strength depends on the effectiveness of the bonding mechanism, and it significantly impacts the sample's ability to

resist separation. Compared to the minimum requirement of 0.15 N/mm^2 stipulated for internal bond strength of particleboards in the Japanese Industrial Standard (JIS-A5908) [41], it can be adjudged that the samples could present satisfactory performance during their service life. Increase in the content of the WWP makes the internal bond strength higher, signifying that the resulting sample is less likely to come apart when subjected to stress perpendicular to its surface. This, in effect, leads to improved structural integrity of the samples as ceilings in building design.

3.4 Feasibility and Benefits of the Research Undertaking

The possibility of achieving self-bonding during fabrication of the samples in this research depends solely on the types of waste materials utilized, production condition, and compaction (pressure applied). Clearly, the materials used (WNP and WWP) are fibers containing hemicellulose and lignin in addition to cellulose. Lignin exhibits gluing behavior and has a structure skeleton consisting of phenylpropene working as a rigid support in the cell walls of the fibers. Also, hemicellulose is an oligomeric mixture containing various monosaccharides which adhere to the microfibril surfaces. Under the presence of moisture (a wet condition facilitated by moistening of the materials during the production stage), the chemical activation of lignin and hemicellulose creates resin-like substances. This, plausibly, promotes inter-fiber physical contact and cross-linking as controlled by surface deformability (to determine the area of molecular contact at fiber-fiber physical interaction points) giving rise to interfacial bonding between the WNP and WWP. Due to exclusion of adhesive from the materials mix designs, there is no need for a curing period. This helps to reduce production time and consequently benefits both the environment and economy.

Additionally, the binderless WNP-WWP samples produced are considered as a promising alternative to other structural materials, especially ceilings in buildings due to their advantages such as cost-effectiveness, eco-friendliness, and scalability. Since the production process described in this research is scalable, assorted sizes of the samples can be produced for use in building construction. But because papers/paper products are biodegradable, water-absorbing, and combustible in addition to their tendency to undergo thermal aging, the WNP-WWP ceilings should be applied internally in buildings and also prevented

from exposure to prolonged humidity during their service life in order to enhance their durability.

Conclusion

This research has revealed that WNP and WWP differ in the proportions of their lignocellulosic fractions, signifying that they are suitable pairs for formulation of composite panels. The bulk density (587.0 kgm^{-3}) was obtained with 100.0% WNP highlighting that being of low densities, the samples could offer the advantage of reducing dead loads if applied as ceiling boards. Better improvements in heat restriction ability were observed with increasing proportions of the WNP reducing thermal conductivity from 0.0835 $Wm^{-1}K^{-1}$ to 0.0628 $Wm^{-1}K^{-1}$ when utilized up to 100% thus signifying the samples' effectiveness in ensuring satisfactory thermal comfort in buildings. More so, the nailability of the samples was found to be 100.0%, meaning that they can withstand nail penetration during their installation as ceilings. While the WNP enhanced thermal insulation performance, the WWP was presented greater tendency for better strength, leading to a balance at 50.0% loading levels yielding samples with thickness swelling, flexural strength, and internal bond strength of 23.58%, 1.276 N/mm^2, and 0.181 N/mm^2 respectively which are acceptable for interior applications of structural materials.

References

[1] U.W. Robert, S.E. Etuk, et al., Discov. Mater., **5**, 19 (2025).

[2] M. Roestamy, A. Martin, IJASOS, **5**, 967 (2019).

[3] V.A. Arowoiya, A.O. Onososen, et al., Buildings, **14**, 1310 (2024).

[4] U.W. Robert, S.E. Etuk, et al., Int. J. Thermophys., **42**, 1 (2021).

[5] J. Rocha, S. Oliveira, et al., *One Health, Chapter 8 – Climate Change and its impacts on health, environment and economy,* (Academic Press, 2022).

[6] U.W. Robert, S.E. Etuk, et al., Int. J. Thermophys., **43**, 74 (2022).

[7] O.B. Ezeudu, J.C. Agunwamba, et al., Resources, **53**, 53. (2019).

[8] Z. Ma, Y. Yang, et al., Environ. Sci. Technol., **55**, 8492 (2021).

[9] B.T. Amena, N. Hossain, J. Compos. Sci., **8**, 176. (2024).

[10] U.S. Okorie, U.W. Robert, et al., Journal of Renewable Energy and Mechanics, **3**, 32 (2020).

[11] A.H.I. Ibrahim, P.A.S. Ern¸ et al., Progress in Engineering Application and Technology, **1**, 104 (2020).

[12] U.W. Robert, S.E. Etuk, et al., Structure and Environment, **15**, 38 (2023).

[13] G.P. Umoren, U.S. Okorie, et al., Science, Engineering and Technology, **3**, 75 (2023).

[14] M. Amberber, Y.Addis., J. Waste Resour., **7**, 290 (2017).

[15] U.W. Robert, S.E. Etuk, et al., Polytechnica, **4**, 97 (2021).

[16] M. Xiu, S. Stevanovic, et al., Environmental Research, **167**, 536 (2018).

[17] C. Sassanelli, A. Urbinati, et al., Computers in industry, **120**, 103245 (2020).

[18] Y. Zhang, Y. Chen, et al., ACS Sustain. Chem. Eng., **10**, 15538 (2022).

[19] T. Ju, L. Liu, et al., ACS Sustain. Chem. Eng., **12**, 13316 (2024).

[20] I.P. Nitu, M. Shams, et al., Handbook of Ecomaterials. *Development of Binderless Composites from Different Nonwood Lignocellulosic Materials: Overview,* (Springer, Cham, 2018).

[21] A.I. Anukam, J. Berghel, et al., J. Wood Chem. Technol., **40**, 15 (2020).

[22] U.W. Robert, S.E. Etuk, et al., Engineering and Technology Journal, **42**, 430 (2024).

[23] U.W. Robert, S.E. Etuk, et al, Iraqi Journal of Science, **60**, 1704 (2019).

[24] S.E. Etuk, U.W. Robert, et al, Advances in Materials Science, **23**, 19 (2023).

[25] U.W. Robert, S.E. Etuk, et al., Int. J. Lightweight Mater. Manuf., **7**, 631 (2024).

[26] U. Robert, S.E. Etuk, et al., J. Sci. Technol., **2**, 1 (2022).

[27] U.W. Robert, S.E. Etuk, et al., Int. J. Thermophys., **42**, 113 (2021).

[28] S.E. Etuk, U.W. Robert, et al, Beni-Suef University Journal of Basic and Applied Sciences, **9**, 1 (2020).

[29] A.U. Anonaba, F.C. Eze, et al, Engineering and Technology Journal, **8**, (2024).

[30] S.E. Etuk, U.W. Robert, et al, Journal of Oil Palm Research, **35**, 448 (2022).

[31] A.S. Vasudeva, Modern Engineering Physics, 6th Revised edn., *Part II*, S. (Chand & Company Ltd, Ram Nagar, New Delhi, 2013).

[32] U.W. Robert, S.E. Etuk, et al., Imam Journal of Applied Sciences, **5**, 68 (2020).

[33] G.P. Umoren, A.O. Udo, et al, Researchers Journal of Science and Technology, **3**, 1 (2023).

[34] J.B. Emah, A.A. Edema, et al., J. Sustain. Constr. Mater. Technol., **9**, (2024).

[35] ASTM D 1037, Standard test methods for evaluating properties of wood-base fiber and particle panel materials. ASTM International, West Conshohocken, PA. (2020).

[36] U.W. Robert, S.E. Etuk, et al., Environmental Technology & Innovation, **24**, 101869 (2021).

[37] A. Ferrandez, M.T. Ferrandez, et al., Agronomy, **12**, 1387 (2022).

[38] S.J. Mitchual, P. Mensah, et al., Materials Science and Applications, **11**,817 (2020).

[39] E.R.K. Rajput, Heat and mass transfer, 6th Revised edn., (S. Chand and Company PVT Ltd, p.15, 2015).

[40] E.E. Nduduba, D.C. Nwobodo, et al., International Journal of Engineering Research and Applications, **5**, 29 (2015).

[41] JIS A5908, Japanese Industrial Standard – Particleboards, (Published by Japanese Standard Association, 2022).